Progressive Amplitude Fatigue Performance of Additively Manufactured Stainless Steel Superalloy

Sanna F. Siddiqui, Krystal Rivera, Isha Ruiz-Candelario, and Ali P. Gordon

Abstract Advances in aerospace component manufacturing design are being achieved through the additive manufacturing (AM) technology. Variations in cyclic loads (i.e. variable amplitude fatigue) is a common phenomenon experienced by aerospace components during in-service use, hence the need for AM components to withstand fatigue failure under these conditions. This study has performed progressive strain amplitude fatigue tests at increasing strain ranges with the intent to capture the fatigue failure life, hardening/softening response, and fracture response of as-built direct metal laser sintered (DMLS) Stainless Steel GP1. Preliminary results indicate fatigue failure in specimens prior to reaching strain ranges where plasticity effects become more pronounced. Also, evident is variation in cyclic softening/hardening response to stabilization at elastic versus plastic strain ranges. Scanning electron microscopy was used to identify the precursors for fatigue crack initiation and propagation under progressive amplitude fatigue loading.

Keywords Variable amplitude fatigue · Additive manufacturing · Stainless steel GP1

Introduction

Additive manufacturing (AM) has shown to be advantageous for the aerospace industry because it allows for rapid prototyping and design flexibility, facilitating the manufacturing of complex geometries [1]. To date, studies have primarily investigated the axial, torsional, and rotating bending fatigue performance of AM stainless steel alloys [2–6]. It was determined that one of the major factors affecting fatigue life are defects directly related to the manufacturing process, such as voids and surface

S. F. Siddiqui (✉) · K. Rivera · I. Ruiz-Candelario
Department of Mechanical Engineering, Florida Polytechnic University, Lakeland, FL, USA
e-mail: ssiddiqui@floridapoly.edu

A. P. Gordon
Department of Mechanical and Aerospace Engineering, University of Central Florida, Orlando, FL, USA

roughness [1–3, 7–12], resulting in fatigue life for AM specimens to be significantly less than for their wrought counterparts [2, 9–13]. These defects have been shown to be reduced by post-processing, positively impacting fatigue life [1, 2, 10–12].

During in-service operation, aerospace components are also subjected to variable amplitude (VA) fatigue loading conditions, necessitating the design of AM components to withstand these loading conditions [7, 14–16]. Unlike constant amplitude fatigue, where all load cycles are identical, in VA fatigue, load amplitudes and/or mean stresses may change at regular intervals, impacting both fatigue crack growth and cyclic plasticity [17, 18]. Tensile mean stress overloads in VA have been shown to contribute to fracture [17]. Variable amplitude fatigue performance has been reported for additively manufactured Ti-6Al-4V and stainless steel 15-5PH [7, 14]. An investigation into the variable amplitude fatigue performance of laser sintered versus electron beam melted (EBM) as-built Ti-6Al-4V has revealed that the rough surface contributed to a lower fatigue strength for this material [7]. It was further shown that the cumulative damage approach produced similar findings between the predicted and experimental VA life of this alloy [7]. A comparison between the predicted fatigue cycles under the cumulative damage approach versus experimental testing has been reported for laser-based powder bed fusion produced 15-5 PH stainless steel parts, under both zero and tensile mean stresses [14]. Multiple crack initiation sites were reported for VA under tensile mean stress as opposed to zero mean stress, for which a distinct crack initiation site was observed [14].

The proposed study is unique in that it provides preliminary findings into the progressive amplitude fatigue performance of additively manufactured stainless steel (SS) GP1, which has a chemical composition similar to stainless steel 17-4PH [19], but varies in mechanical performance as reported in other studies [20–22]. Progressive strain amplitude fatigue tests are performed at increasing strain ranges for as-built direct metal laser sintered (DMLS) SS GP1, in order determine its fatigue failure life, hardening/softening response, and identify the role of AM induced defects on the resulting fatigue fracture response.

Experimental Design

To assess the progressive amplitude fatigue performance of as-built additively manufactured stainless steel (SS) GP1, specimens of horizontal build orientation (X, Y, and XY45) were manufactured using the EOS M280 direct metal laser sintering (DMLS) system in a nitrogen environment with a layer thickness of 20 µm. EOS-optimized processing parameters were used to manufacture the specimen design shown in Fig. 1, which were not subject to heat-treatment. The as-built specimens boxed support structure were removed with conventional hand tools, and the gripping sections of the specimens were machined from the manufactured diameter of 0.625 in to 0.5 in prior to progressive amplitude fatigue testing. Further details regarding specimen preparation prior to fatigue testing can be found in [6].
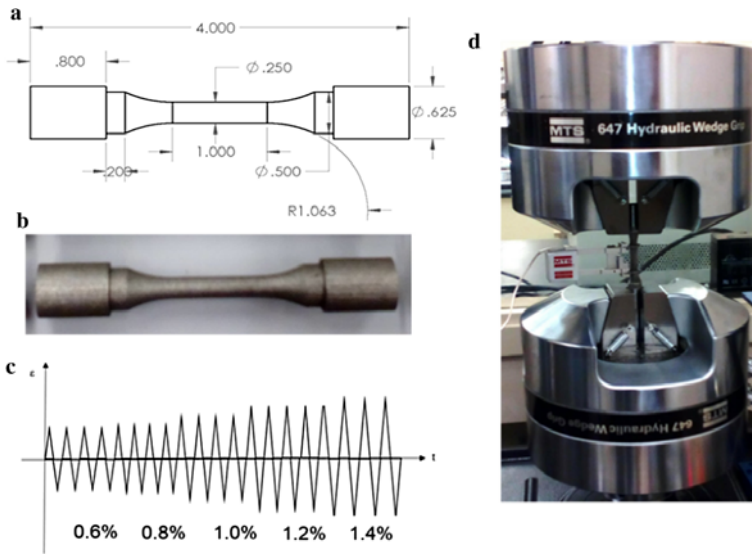
Fig. 1 **a** Sample geometry (dimensions in inches), **b** as-built DMLS Stainless Steel GP1 prior to machining gripping section, **c** proportional amplitude fatigue test sequence, **d** experimental setup [6, 20]. (Color figure online)

Progressive strain amplitude fatigue testing was performed to assess the increase in strain range (elasticity, equivalent amounts of elasticity and plasticity, and plasticity) on crack initiation/propagation in as-built AM test specimens [6]. Strain-control progressive amplitude fatigue tests ($R_\varepsilon = -1$) were performed using the MTS LandMark 793 servohydraulic system at room temperature with a strain rate of 10^{-3} (mm/mm/s) and sampling rate of 25 Hz [6]. In an effort to identify the cyclic stress–strain response of DMLS SS GP1, testing was performed at strain ranges of $\Delta\varepsilon = 0.6\%$, $\Delta\varepsilon = 0.8\%$, $\Delta\varepsilon = 1.0\%$, $\Delta\varepsilon = 1.2\%$, and $\Delta\varepsilon = 1.4\%$, as shown in Fig. 1. Testing was performed for a set number of cycles (~100) at each strain range, which was identified from preliminary testing to approximately achieve stabilization of hysteresis loops at each strain range. In addition to determining the total fatigue failure life, hardening/softening response at each strain range, hysteresis deformation response, and fracture mechanics under progressive amplitude fatigue conditions were explored. The Hitachi SU 3500 scanning electron microscope (SEM) was used to characterize the fracture surfaces (i.e. crack initiation and propagation) of DMLS SS GP1 samples due to progressive amplitude fatigue loading conditions, including defects at the microstructural level contributing to observed fracture response. The sample was mounted onto a 51 mm specimen stub, using double-sided conductive adhesive tape [23], and imaged using secondary electron (SE) mode at varying magnifications. The resulting fracture surfaces and associated key features observed are presented and discussed in the results and discussion section.

Results and Discussion

Progressive amplitude fatigue cycling of DMLS stainless steel GP1 specimens resulted in the following stress–life plot shown in Fig. 2. Given that the specimens were manufactured in the horizontal build orientation (X, Y or XY45), the progressive amplitude fatigue response at each strain range is similar. Hence, suggesting that manufacturing at build orientations in the horizontal plane plays a limited role in impacting progressive amplitude fatigue performance. Also, evident from Fig. 2 is the presence of hardening and softening within each strain range. At a highly elastic strain range of $\Delta\varepsilon = 0.6\%$, softening is evident to stabilization. However, at strain ranges where plasticity is more pronounced or equivalent amounts of elasticity and plasticity are present (i.e. $\Delta\varepsilon = 1.0\%$ and $\Delta\varepsilon = 1.2\%$), cyclic hardening is observed to stabilization. The rate of cyclic hardening appears to increase with strain range. This may suggest that at strain ranges where plasticity effects become more pronounced, the hardening behavior may be attributed to a strain-induced austenite to martensite phase transformation, as suggested in other studies on additively manufactured stainless steel 17-4PH [2, 6]. Future work through x-ray diffraction techniques will be used to capture phase transformations to confirm this finding.

An assessment of fatigue life under progressive amplitude fatigue loading is also captured in Fig. 2. Here, it is evident that all specimens regardless of build orientation in the xy plane fractured at a strain range of $\Delta\varepsilon = 1.4\%$. On average, specimens fractured after approximately 416 cycles, after cycling for 100 cycles at strain ranges of $\Delta\varepsilon = 0.6\%$, $\Delta\varepsilon = 0.8\%$, $\Delta\varepsilon = 1.0\%$, and $\Delta\varepsilon = 1.2\%$. The increase in strain range, in which plasticity effects became more pronounced, is suggested to accelerate fatigue crack growth resulting in specimen failure upon reaching a strain range of $\Delta\varepsilon = 1.4\%$. It is suggested that defects at the microstructural level, such as the as-built surface roughness, contributed to fatigue crack initiation and accelerated crack propagation. This is further explored through SEM micrographic imaging.
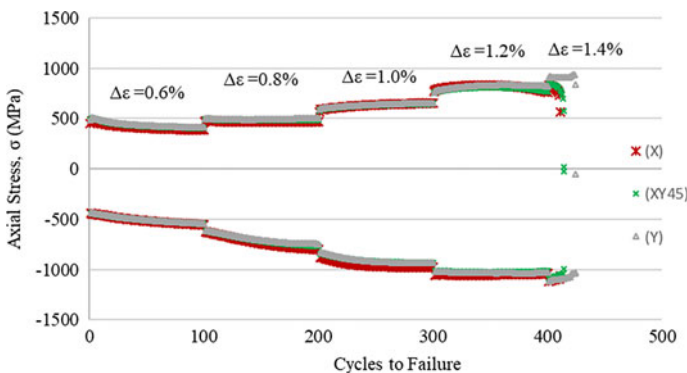

Fig. 2 Stress–life of as-built DMLS SS GP1, of varying build orientation, under progressive amplitude fatigue testing from $\Delta\varepsilon = 0.6\%$ to $\Delta\varepsilon = 1.4\%$. (Color figure online)

Nevertheless, it would appear that progressive amplitude fatigue testing is detrimental to the life of as-built DMLS SS GP1 manufactured in the horizontal build plane [6]; however, as these results are based upon a small sample size, future work will be done to confirm these findings.

An analysis of the fracture surface of DMLS SS GP1 through scanning electron microscopy (SEM) is presented in Fig. 3. The overall fracture surface reveals multiple crack initiation sites near the surface and evidence of striation patterns indicating fatigue crack propagation. Internal defects, such as regions of powder particles and lack of fusion, can also be observed from the SEM micrograph images. This has been shown in recent studies on additively manufactured Ti-6Al-4V and SS 15-5PH subject to variable amplitude fatigue loading as well [7, 14]. Overall, fatigue cracks under progressive amplitude fatigue loading have been found to initiate at un-melted powder particles near the as-built rough surface.

To further evaluate the cyclic deformation response of DMLS SS GP1 under progressive amplitude fatigue loading, the first and stabilized cycles at each strain range are presented in Fig. 4. Since findings across build orientation in the xy plane were similar, as discussed earlier, the hysteresis curves presented are only for the (Y) build orientation. As stabilization occurred after cycling at ~ 100 cycles for each strain range, the last cycle prior to increase in strain range has been considered as the stabilized cycle within these plots. Given that all specimens failed under cycling at a
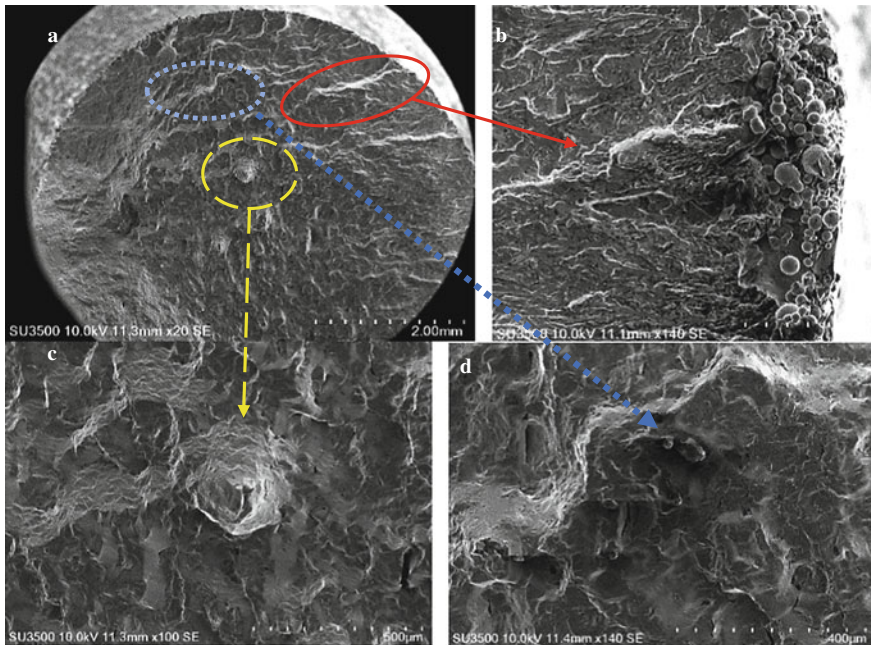
Fig. 3 **a** Complete fracture surface, **b** crack initiation site at un-melted powder particles near surface, **c** and **d** presence of un-melted powder particles and regions of lack of fusion. (Color figure online)
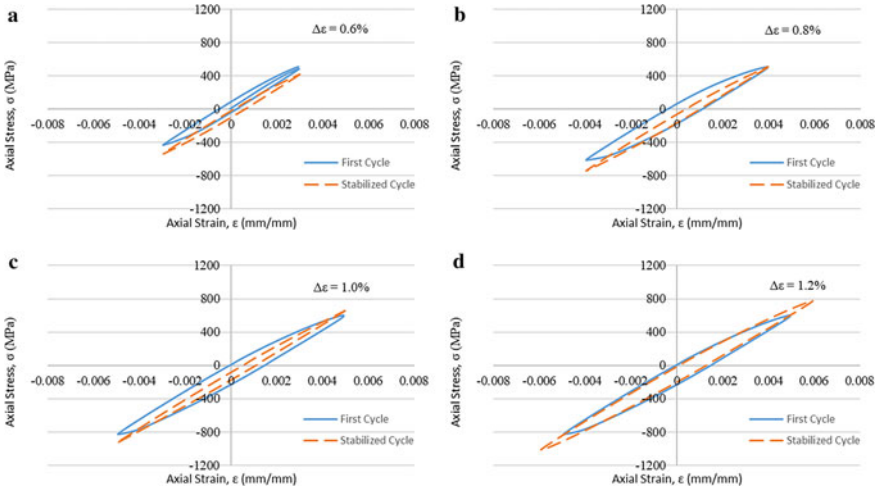
Fig. 4 Hysteresis deformation response (first cycle and stabilized cycle) at each strain range, **a** $\Delta\varepsilon$ = 0.6%, **b** $\Delta\varepsilon$ = 0.8%, **c** $\Delta\varepsilon$ = 1.0%, and **d** $\Delta\varepsilon$ = 1.2%. (Color figure online)

strain range of $\Delta\varepsilon = 1.4\%$, the hysteresis curves for the first and stabilized cycles are plotted up to a strain range of $\Delta\varepsilon = 1.2\%$. An analysis of the hysteresis curves reveals minimum plastic strain range as compared with elastic strain range. A compressive mean stress is also evident from the plots. Evident from both the stress–life plots and analysis of hysteresis curves is cyclic softening at $\Delta\varepsilon = 0.6\%$ and slight cyclic hardening at $\Delta\varepsilon = 0.8\%$, following by considerable cyclic hardening at $\Delta\varepsilon = 1.0$ and 1.2%.

Conclusions and Future Work

This study has investigated the role of progressive strain amplitude fatigue on the life, softening/hardening response, and fracture response of DMLS SS GP1. Specimens were subject to cycling at strain ranges of $\Delta\varepsilon = 0.6\%$ to $\Delta\varepsilon = 1.4\%$, under completed reversed ($R_\varepsilon = -1$) conditions, from which the following conclusions were drawn:

- At strain ranges where plasticity is more pronounced or equivalent amounts of elasticity and plasticity are present (i.e. $\Delta\varepsilon = 1.0\%$ and $\Delta\varepsilon = 1.2\%$), cyclic hardening is observed to stabilization. The rate of cyclic hardening appears to increase with strain range. Cyclic softening is observed at a strain range of $\Delta\varepsilon = 0.6\%$.
- When subject to progressive strain amplitude fatigue loading, from $\Delta\varepsilon = 0.6\%$ to $\Delta\varepsilon = 1.4\%$, for 100 cycles at each strain range, DMLS SS GP1 manufactured in the horizontal build plane is found to fracture during cycling at a strain range of $\Delta\varepsilon = 1.4\%$.

- Specimens manufactured in the horizontal build plane (X, Y and XY45 build orientations) yielded similar performance under progressive amplitude fatigue testing.
- SEM micrographic images reveal multiple fatigue cracks initiating at regions of un-melted powder particles near the as-built rough surface.

Future work will explore the role of build orientation on the progressive amplitude fatigue performance of DMLS SS GP1, providing insight into the variation in cyclic stress–strain curve with build orientation.

References

1. Frazier WE (2014) Metal additive manufacturing: a review. J Mater Eng Perform 23:1917–1928. https://doi.org/10.1007/s11665-014-0958-z
2. Yahollahi A, Shansaei N, Thompson S, Elwany A, Bian L (2017) Effects of building orientation and heat treatment on fatigue behavior of selective laser melted 17-4 PH stainless steel. Int J Fatigue 94:218–235. https://doi.org/10.1016/j.ijfatigue.2016.03.014
3. Yu C, Zhang P, Zhang Z, Liu W (2020) Microstructure and fatigue behavior of laser-powder bed fusion austenitic stainless steel. J Mater Sci Technol 46:191–200. https://doi.org/10.1016/j.jmst.2019.08.047
4. Ochi Y, Matsumura T, Masaki K, Yoshida S (2002) High-cycle rotating bending fatigue property in very long-life regime of high-strength steels. Fatigue Fract Eng Mater Struct 25:823–830. https://doi.org/10.1046/j.1460-2695.2002.00575.x
5. Siddiqui SF, Irmak F, Fasoro AA, Gordon AP (2020) Torsional fatigue failure of additively manufactured stainless steel of reduced specimen size. JOM 72:440–447. https://doi.org/10.1007/s11837-019-03842-9
6. Siddiqui SF (2018) Characterization of anisotropic mechanical performance of as-built additively manufactured metals, Ph.D. Dissertation, University of Central Florida
7. Kahlin M, Ansell H, Moverare J (2017) Fatigue behavior of additive manufactured Ti6Al4V, with as-built surfaces, exposed to variable amplitude loading. Int J Fatigue 103:353–362. https://doi.org/10.1016/j.ijfatigue.2017.06.023
8. Yadollahi A, Shamsaei N (2017) Additive manufacturing of fatigue resistant materials: challenges and opportunities. Int J Fatigue 98:14–31. https://doi.org/10.1016/j.ijfatigue.2017.01.001
9. Yadollahi A, Shamsaei N, Thompson SM, Elwany A, Bian L, Mahmoudi M (2015) Fatigue behavior of selective laser melted 17–4 PH Stainless Steel
10. Bajaj P, Hariharan A, Kini A, Kürnsteiner P, Raabe D, Jagle EA (2019) Steels in additive manufacturing: a review of their microstructure and properties. Mater Sci Eng 772. https://doi.org/10.1016/j.msea.2019.138633
11. Yusuf SM, Cutler S, Gao N (2019) Review: the impact of metal additive manufacturing on the aerospace industry. Metals 9. https://doi.org/10.3390/met9121286
12. Carneiro L, Jalalahmadi B, Ashtekar A, Jiang Y (2019) Cyclic deformation and fatigue behavior of additively manufactured 17–4 PH stainless steel. Int J Fatigue 123:22–30. https://doi.org/10.1016/j.ijfatigue.2019.02.006

13. Rack HJ, Kalish D (1974) The strength, fracture toughness, and low cycle fatigue behavior of 17-4 PH stainless steel. Metall Mater Trans 5:1595–1605. https://doi.org/10.1007/BF02646331

14. Sarkar S, Kumar CS, Nath AK (2018) Investigation on the mode of failures and fatigue life of laser-based powder bed fusion produced stainless steel parts under variable amplitude loading conditions. Add Manuf. https://doi.org/10.1016/j.addma.2018.10.044

15. Schijve Jaap (2009) Fatigue under variable-amplitude loading. Fatigue of structures and materials. Springer, Dordrecht, pp 296–297

16. Kardomateas GA, Geubelle PH (2010) Fatigue and fracture mechanics in aerospace structures. Encycl Aerosp Eng **3**. https://doi.org/10.1002/9780470686652.eae142

17. Marquis GB (2011) Fatigue assessment methods for variable amplitude loading of welded structures. In: Fracture and fatigue of welded joints and structures. pp 208–238. https://doi.org/10.1533/9780857092502.2.208

18. Pommier S (2003) Cyclic plasticity and variable amplitude fatigue. Int J Fatigue 25:983–997. https://doi.org/10.1016/S0142-1123(03)00137-3

19. EOS GmbH-Electro Optical Systems. Material Data Sheet: EOS Stainless Steel GP1 for EOSINT M 270. 1–5

20. Siddiqui SF, Fasoro AA, Cole C, Gordon AP (2019) Mechanical characterization and modeling of direct metal laser sintered stainless steel GP1, J Eng Mater Technol 141(3)

21. Facchini L, Vicente N, Lonardelli I, Magalini E, Robotti P, Molinari A (2010) Metastable austenite in 17-4 precipitation-hardening stainless steel produced by selective laser melting. Adv Eng Mater 12(3):184–188

22. Luecke WE, Slotwinski JA (2014) Mechanical properties of austenitic stainless steel made by additive manufacturing. J Res Natl Inst Stand Technol 119:398–418

23. Hitachi High-Technologies Corporations (2014) Model SU3500 Scanning Electron Microscope: Easy operation guide, Japan